Advanced Powder Technology 26 (2015) 1123–1133

Contents lists available at ScienceDirect

Advanced Powder Technology

journal homepage: www.elsevier.com/locate/apt

Original Research Paper

Characterization of nano-silica prepared from local silica sand and its application in cement mortar using optimization technique

Najat J. Saleh, Raheek I. Ibrahim *, Ali D. Salman

Chemical Engineering Department, University of Technology, Alsinaa Street 52, Baghdad, Iraq

ARTICLE INFO

Article history:
Received 6 October 2014
Received in revised form 5 April 2015
Accepted 18 May 2015
Available online 3 June 2015

Keywords:
Silica nanoparticle
Silica sand
Ball milling
Optimization
Portland cement mortars

ABSTRACT

The objective of this work is to prepare, and characterize silica nanoparticles (NS) for the first time from Ardma silica sand, which is obtained from Anbar province in the west of Iraq. The procedure suggests using a combination of ball milling and heating process, then evaluating the influence of (NS) addition on mechanical properties (compressive strength and splitting tensile strength) of mortar mixture to improve its characteristics. Optimization of the operating variables (nanosilica particle size, and percentage of addition) involved using (WinQSB) and (Statistica) software to predict the optimum conditions. Samples have good SiO_2 value of about 99.2% increased up to 99.83% after leaching with sulfuric acid. The high purity silica sand was milled for 30–50 h to produce nanoparticle silica with average particle size of 50 nm. By means of TEM, SEM, AFM, and PSA characterization, these nanoparticles look like spherical particles and have irregular shapes with clusters, the range of their external diameters is (30–100) nm. These nanoparticles silica have a good possibility to be applied as an additive material to produce ultra high performance concrete. According to our knowledge, there is no previous work focusing on preparing of silica nanoparticles from Ardama silica sand, and used to improve mechanical properties of cement mortar using optimization technique. Optimization results proved that an improvement in compressive strength of 29.889% occurred under optimum conditions (6% adding percent and 50 nm particle size), while tensile strength was 22.863% under optimum conditions (8% adding percent and 50 nm particle size) at 28 day age.

1. Introduction

Nanoparticles of silica sand have been researched progressively and produced due to their unique features as a result of size reduction. Silica sand nanoparticles have proved to be a very effective additive to concrete by improving durability, mechanical properties and workability to produce high performance concretes. Nano-silica is also used as effective additive to polymers to improve durability, strength, and flexibility. Nano-silica particles are widely produced by chemical processes. However, chemical synthesis of NS produces high contamination in the final products. As the demand is increasing for higher NS purity, contamination is expected at the minimum level. Other than chemical synthesis, other processes such as precipitation, vaporization at high temperature, sol–gel process, high speed vertical rotating mill, and planetary ball mill are among the most commonly used methods to produce silica sand nanoparticles. It is expected that the technique will be able to produce high purity silica sand nanoparticles of less than 100 nm consistently. In the last decades, the employment of NS in concrete has changed it to have better mechanical properties, initializing a great vision to the concrete erections [1]. Nano-scale substances have a great impact on concrete mixtures in order to their higher surface area. A lot of research used various nano materials to show their effect on the concrete. One of the main interest is on NS, this has been attributed to its Pozzolanic characteristics [2].

For NS, the Pozzolanic reaction is more apparent than in silica fume. NS has the ability to react with calcium hydroxide $Ca(OH)_2$ crystals, which are ordered in the interfacial transition zone (ITZ) is among consolidated cement confection and aggregates, and generates a C–S–H gel. Consequently, the volume and quantity of calcium hydroxide are characterized by reduction, and the strength of the reinforced cement developed [3]. Ball milling is one of the wide spread process to produce a fine powder in micro or nano scales [4]. It is useful for grinding whole types of materials [5,6]. It has showed to be unsophisticated and prosperous procedure to get huge amounts of nanoscale materials [7]. Thus, this study focuses on preparation of silica sand nanoparticles from Ardama

* Corresponding author.
E-mail address: doctorraheek@yahoo.com (R.I. Ibrahim).

http://dx.doi.org/10.1016/j.apt.2015.05.008

silica sand using integrated process consisting of ball milling and heating process in order to produce ultra fine and high purity NS, then characterize the product by means of TEM, SEM, AFM, and PSA to insure it reaches a nano-scale. Because there is no present work concentrating on this silica sand nanoparticles conduct inside the cement mortar, this study has optimized the operating parameters like NS particle size and percentage of addition to the cement mortar, using experimental design procedure and utilizing a second order polynomial model equations, the optimization technique employed is (WinQSB) and (Statistica) software used to analyze the developed model equation and predict the optimum conditions, furthermore, the experimental validation of proposed model is also involved.

2. Materials and method

2.1. Preparation of silica nanoparticles

Natural silica sand was taken from Ardma location at Anbar province in western Iraq. The silica sand was first washed to remove impurities. Upgrading of silica process was carried out by using acid leaching process to reduce metal impurities (especially the iron oxides and aluminum oxides) content in the final product, followed by water washing after that, it was dried in an oven at 120 °C for 1 h. Then, the sand was put in a Sieve Shaker to produce a size of 300 μm. The micro-silica sand (MS) was then entered the ball mill simultaneously with the grinding balls for a period of 2 h, then sand was sent to mesh for the size lower than 300 μm in order to remove impurities and severe clusters that originated during milling process, dried again in an oven at 120 °C for 1 h. The meshing and drying are frequently done every 2 h of milling while attaining the total time of 10 h. The mesh sizes employed were 600 μm, 300 μm, 140 μm, and 100 μm. After the 10 h of milling; the ball-milled silica sand was tested using Malvern Instruments Master size 2000 particle size analyzer.

2.2. Preparation of cement mortar specimens

2.2.1. Mix proportions

Thirty mortar mixtures were made for every test of compressive and tensile strengths included in this study, ten experiments were to be carried out for every curing age in sequence according to experimental design. All the cement mortars had a water-to-cementitious materials ratio (w/c) of 0.48 and a sand-to-cementitious materials ratio of 1:3 (one part of the Ordinary Portland cement (OPC) and 3 parts of sand) according to ASTM specifications (C109) [8]. Percentage of the NS varied from 0%, 2%, 6%, to 10% by mass of the cementitious materials. Mortars with NS were compared with that the control mixture to evaluate the influence of dosage and particle size of the (NS). Specifications of mixing attributions of cement mortars are shown in Table 1. The initial band represents the control mortar sample (without NS), while the others represent the addition ratios of NS to cement mortar as 2%, 6%, and 10% by weight.

2.2.2. Specimen preparation, curing, and testing

To prepare cement mortar mixtures solid materials (fine aggregate and ordinary Portland cement) were dry mixed first in a Hobart mixer (mechanical mixing) at an ambient temperature of about 30 °C. NS and water were mixed by using ultrasonic mixer with 750 Watts power input for 5 min. The sonicated mixture was then mixed in a Hobart mixer, and mixed for 1 min at low speed. For each mortar mixture, after that, 2 × 4 inches cylindrical specimens were cast for compressive and tensile strength tests according to ASTM (C780-002). The molded specimens were covered with wet burlap for the first 24 h to prevent moisture loss. After demolding, the specimens were cured in a fog room at a temperature of about 30 °C until the time of testing. Compressive and tensile strengths of the mortars were determined at 7, 14, and 28 days according to ASTM C (780-002) [9].

2.3. Equipments used

The specifications of equipment used during the course of the work have been given in Table 2.

2.4. Optimization process and parameters identification

The operating variables such as particle size (X_1), and NS adding percent (X_2), at 7, 14, 28-day aging times, were correlated in non-linear second order model equations (Eq. (1)), for compressive strength and tensile strength of mortar samples which represent the objective function (Y) to be maximized, as in Eq. (1).

$$Y = a_0 + a_1X_1 + a_2X_2 + a_3X_1X_2 + a_4X_1^2 + a_5X_2^2 \cdots \quad (1)$$

the constraints are defined as:

$$a_{11}X_1 + a_{12}X_2 + \cdots a_{1n}X_n(\leqslant, \geqslant, =)b_1 \quad (2)$$

$$a_{21}X_1 + a_{22}X_2 + \cdots a_{2n}X_n(\leqslant, \geqslant, =)b_2 \quad (3)$$

$$a_{m1}X_1 + a_{m2}X_2 + \cdots a_{mn}X_n(\leqslant, \geqslant, =)b_m \quad (4)$$

$X_i \geqslant 0$ $(i = 1,2,\ldots n)$, n = number of variables, m = number of constraints

$$j = 1,2\ldots n, \quad i = 1,2\ldots m$$

The model equations coefficients were estimated using STATISTICA software (version 8.0). The operating variables of the developed model were optimized using WinQSB software (version 1.0) in order to find the optimum values of operating conditions for enhancing the compressive and tensile strengths. Then experimental validation was also involved.

Table 1
Mixing proportion of mortar samples accordant to optimization technique.

Mix ID	Percentage% (NS)	Particle size (nm)	Nano-silica (gm)	Sand (gm)	Cement (gm)	Water (milli-liter)
M0	0	0	0	225	75	36
M1	2	50	1.5	225	73.5	36
M2	10	50	7.5	225	67.5	36
M3	2	110	1.5	225	73.5	36
M4	2	80	1.5	225	73.5	36
M5	6	50	4.5	225	70.5	36
M6	10	80	7.5	225	67.5	36
M7	6	110	4.5	225	70.5	36
M8	10	110	7.5	225	67.5	36
M9	6	80	4.5	225	70.5	36

Table 2
Specifications of equipments used.

Equipment	Specification
Ball mill	250 rpm
Mechanical Shaker, Heidolph	UNIMAX 1010/PROMAX 1020, Germany
Ultrasonic	750 Watt Ultrasonic Processors – VCX Series
pH meter	Hanna 211, Romania
Electrical furnace	(20–500) °C
Compression testing machine	
A. Hydraulic machine	A. 15 ton
B. ELE-Digital series	B. ELE-ACCU-TEK 250.
Mixer for preparation mortar	Hobart mixer – 20 rpm
Mixer for leaching process	(20–100) rpm
Magnetic stirrer	Heidolph – Models MR. Hei-Tec. 40 rpm
X-ray fluorescence spectrometry	Shimadzu 1800
Particle Size Analyzers (PSA)	Malvern Mastersizer 2000
Atomic Force Microscope (AFM)	Angstrom, Scanning Probe Microscope, Advanced Inc, AA 3000A°, USA
X-ray diffraction	XRD-6000, Shimadzu scan range is (10.0–60.0) deg.
Scanning electron microscope (SEM)	Type TESCAN
Transmission electron microscopy (TEM)	CM10 Philips, Netherlands
Brunauer, Emmett and Teller (BET) method by surface area analyzer	Q Surf 1600, USA
The FT-IR instrument	BRUKER, Germany

3. Results and discussion

3.1. Characterization of the silica sand and silica nanoparticles

The results obtained from the optimum leaching of sulfuric acid (H_2SO_4) concentration of 7.5% show the silica percent increased from (99.2%) to (99.83%) of SiO_2 after the leaching process. On the other hand metallic impurities K_2O, Al_2O_3, Fe_2O_3, CaO, and MgO contents have been decreased. For example (Fe_2O_3) slumped from (0.092%) to (0.03%). These results are in good agreement with the results obtained by Wahyudia et al. [10].

The silica nanoparticles obtained from ball milling process were verified by (PSA) particle size analyzer. According to (PSA) silica has successfully been reduced to particle size of 50 nm sized milling within (30) hours. Fig. 1 shows the resulting particle size during the milling process with time.

Atomic force microscope observation identified the diameters of prepared NS. Two different groups of samples were analyzed, the range of first group was (60–120) nm, with average diameter of 88.87 nm and the higher volume percent of particle size was 80 nm after 40 h of milling. The range of second group was (90–170) nm, average diameter of 119.70 nm and higher volume percent of particle size was 110 nm after 50 h of milling as shown in Fig. 2A and B. According to the results of (PSA) and (AFM) the size distribution of particles was in three main different size groups of (NS) (30–100) nm, (60–120) nm and (90–170) nm. Based on the milling pattern, it can be concluded that the mineral

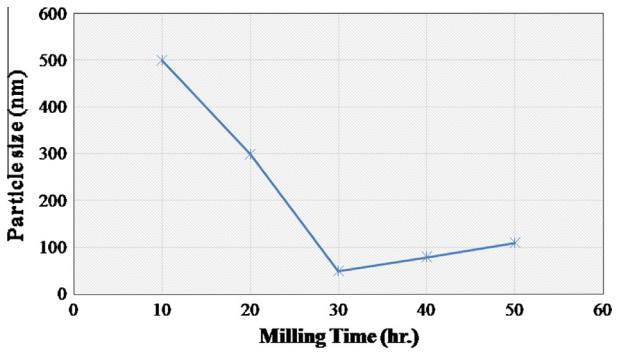

Fig. 1. Particle size of silica sand samples at different milling times according to particle size analyzer.

is brittle and characterized by reduction in particle size first and then agglomeration (clumping) is run with increasing milling time. Agglomeration is the result of Van der Waal forces between particles at the surface.

The SEM images shown in Fig. 3A illustrate morphology, size and distribution of the ball-milled silica (micro-silica) after 10 h of milling. It can be seen that some of SiO_2 particulates which have fused together resulted from constricting action of the ball-milling process. The SEM images shown in Fig. 3B demonstrate ball-milled silica nanoparticles after 30 h of milling, different structures of the (NS) particles including spherical particles and irregular shape particles as well as agglomerates are due to constricting action of the ball-milling process. This vigorous proclivity for agglomeration which subsists in the particles is induced by the Van-der-Waal forces acting between the individual particles. As it can be visually perceived from the results the particle size of NS is not homogeneous and several primary particles seem to cluster or fuse at their faces and range (159, 62, 50) nm. These results are in good agreement with the results obtained by Wahyudia et al. [10].

The TEM image in Fig. 4 shows that various structures of the (NS) particles including irregular shape particles, spherical particles, solid and highly agglomerated in shape are due to Van der Waal force on the particle surface and confirm the solid structure of NS. The range of diameters is (30–100) nm for the sample tested. These results are in good agreement with the results obtained by Ahmad et al. [11].

Fig. 5a and b demonstrate the structural changes and degradation in the treated silica, compared with untreated materials. XRD profile in Fig. 5a shows that, the pattern of white silica sand before fracture demonstrates the presence of a large amount of highly crystalline quartz. The {101} and {100} basal reflections, initially are very strong, a decrease in intensity after smash is shown in Fig. 5b. The reflections {110}, {102} and {200} decrease too but are different from others after mechanical treatment for 30 h. This confirms the structural changes in the treated silica sand, compared to the untreated silica sand before crush. The deformation of structure is reflected in the decrease in peak intensity. The corresponding diffractograms to the lattice planes {100}, {101}, {110}, {102} and {200} are indication of enhancement in the continuous background, which means an increasing concentration of non-crystalline NS in the sample. The loss of crystallinity in the basal diffractions {100} and {110} is due to the amorphization phenomenon. These results are in good agreement with the results obtained by Wang and Forssberg [12].

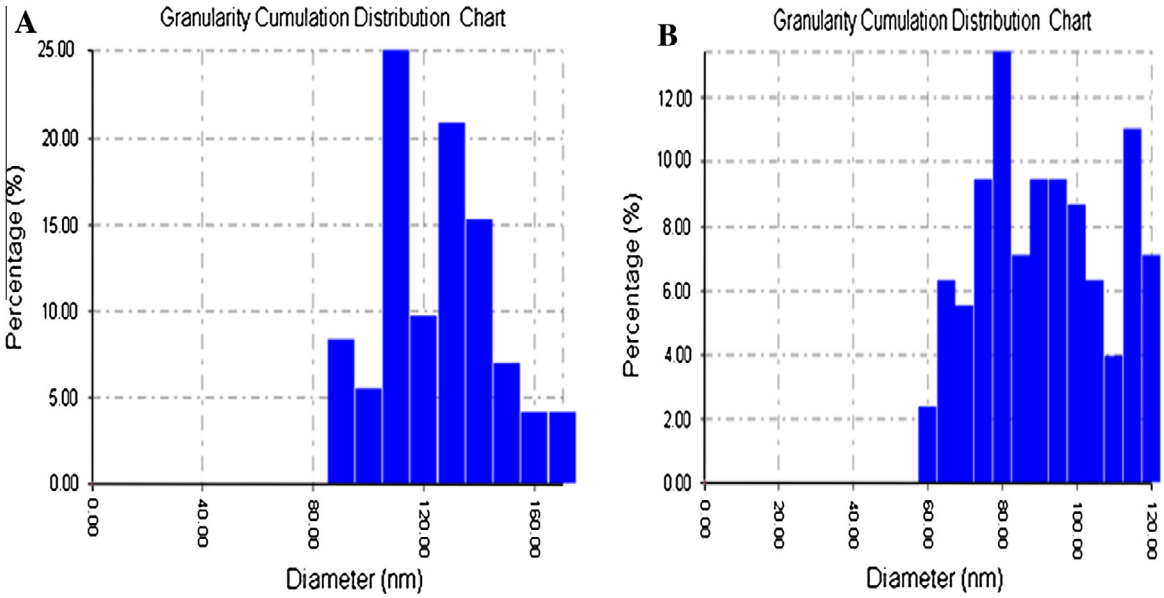

Fig. 2. AFM of prepared (NS): A (90–170) nm, and B (60–120) nm.

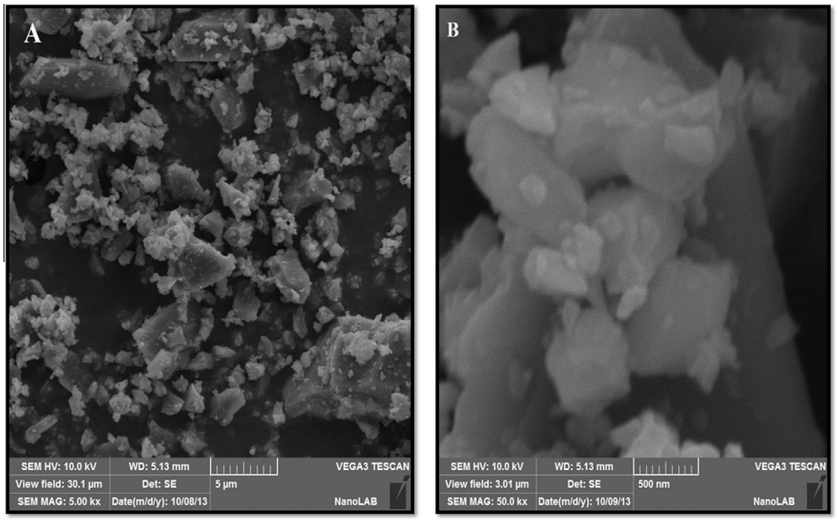

Fig. 3. SEM images: (A) for the ball-milled silica sand (Micro-silica), (B) for the ball-milled silica sand nanoparticles (Nano-silica).

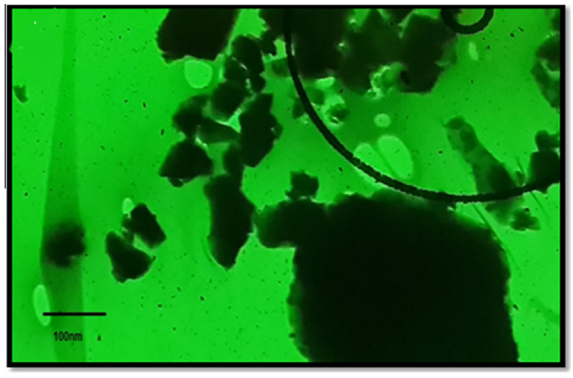

Fig. 4. TEM image for the prepared NS.

The specific surface area (SSA) of the prepared NS groups is determined by the (BET) method. Table 3 shows that the NS has different specific surface areas according to particle size. The smaller particle size group has higher surface area than other groups. These results are in good agreement with the results obtained by Quercia et al. [13].

3.2. Characterization and analysis of cement mortar

3.2.1. SEM observations and microstructure analysis of (CM)

Fig. 6A shows the SEM micrographs of the control mortar mixture at the age of 28 days and demonstrates porous structure that is full of large size pores and the presence of $Ca(OH)_2$ that is over-shadowed. Also it can be seen from the same figures the existence of many CH crystals connected to the C–S–H gel which indicates that the hydration process is not completed and also explains the low records of compressive and tensile strengths for the control mixture. Also, the same photos show that the concentration of the CH is higher than the C–S–H gel concentration and that the CH hydrate needles cover a large area. These results are in good agreement with the results obtained by Singh et al. [14], Belkowitz and Armentrout [15], and Quercia et al. [16].

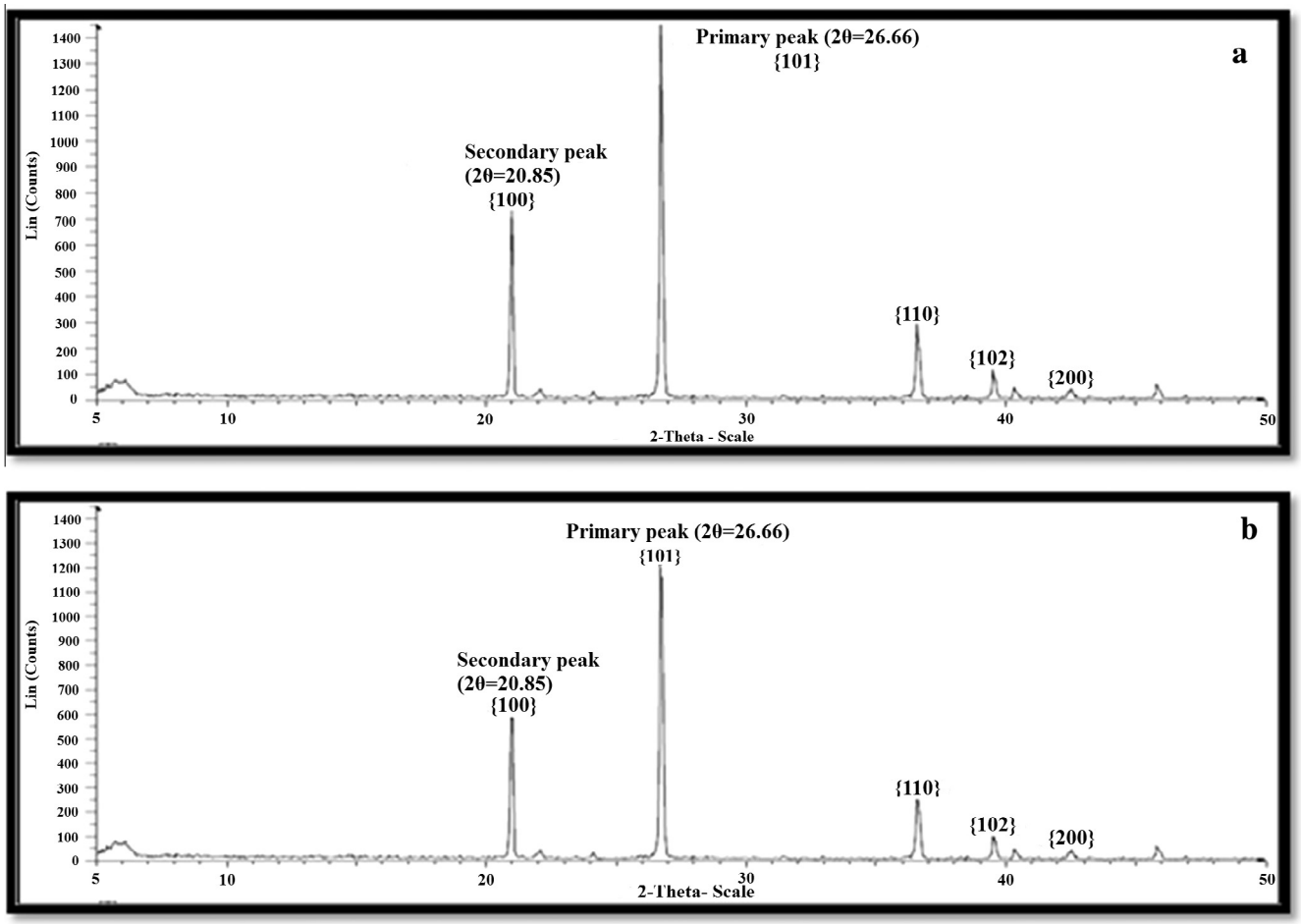

Fig. 5. XRD of (a), silica sand, and (b), nano-silica sand.

Table 3
Physical properties of NS groups consumed.

Groups	SSA (m^2/g)	Particle size group (nm)	Average particle size (nm)
Physical properties			
NS1	40	(30–100)	50
NS2	28.4	(60–120)	80
NS3	18	(90–170)	110

3.2.2. SEM observations and microstructure analysis of NS6 (30–100)

The SEM images of the mortar mixture NS6 (30–100) are shown in Fig. 6B that was prepared with 6% NS of nominal particle size group (30–100) nm. Fig. 6B shows that the microstructure of the cement mortar mixture after incorporating (NS) at the age of 28 days is dense and more organized with a small number of $Ca(OH)_2$ crystals and small sized pores while the control mixture the C–S–H gel existed in the form of clusters lapped and joined together by many CH needles hydrates. It can also be noticed from the same photo that the CH needles are visible and there is a compact structure with the absence of the un-hydrated crystals and voids and is more uniform and homogeneous than that of the (CM) sample which explains the superior compressive strength results. This could be due to the high activity of many particles that promote the pozzolanic reaction to produce more C–S–H gel in order to record high compressive strength at early age which is confirmed by the strength results. NS consumes calcium hydroxide crystals, fills pores to increase the strength, reduces the size of the crystals at the interface zone and transmutes the calcium hydroxide feeble crystals to the C–S–H crystals, and improves the interface zone and cement paste structures. These results are in good agreement with the results obtained by Belkowitz and Armentrout [15], Quercia et al. [16] and Aly et al. [17].

3.2.3. X-ray diffraction of cement mortar (XRD)

XRD analyses were conducted to investigate the activity and potential of incorporating NS on selective mortar specimens after 28 days of hydration. The samples were cured for 28 days of hydration before being subjected to XRD technique. It is obvious from XRD profiles that the CH peak is almost decreased with the addition of NS, while the same is significantly present in control mixture. It is therefore inferred from Fig. 7A and B that, NS reacts with CH produced during the hydration process. The pozzolanic reactivity of NS at early stage of hydration is significantly high and improves the microstructure of cementitious system, thereby enhancing the mechanical properties of the cementitious materials. For comparison, the peaks of CH at 18° and 47° (2θ) have been selected as shown in Fig. 7A, a sharp peak in CH is observed in the control mixture representing the pure hydration product (CH), which is released from the hydration of cement. Evidently, the intensity of the CH peak is decreased due to adding NS as a cement replacement, which reflects the consumption of CH by pozzolanic reaction as shown in Fig. 7B. In agreement with the SEM results, which explain the absence of the un-hydrated crystals (needles) and voids, in addition, more uniform and homogeneous mixtures have been obtained than from the (CM) sample. These results are in good agreement with the results obtained by Quercia et al. [16] and Aly et al. [17].

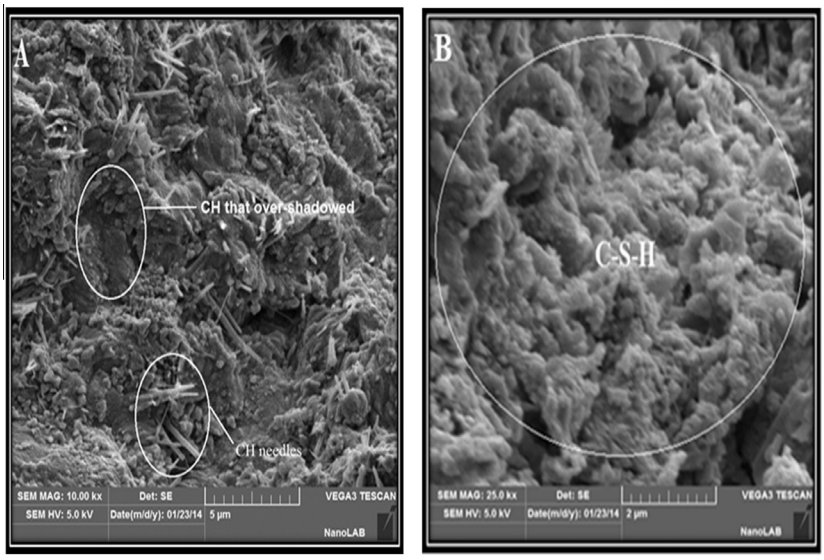

Fig. 6. SEM images of cement mortar (A), before incorporating NS, and (B) after incorporating NS at 28 days age.

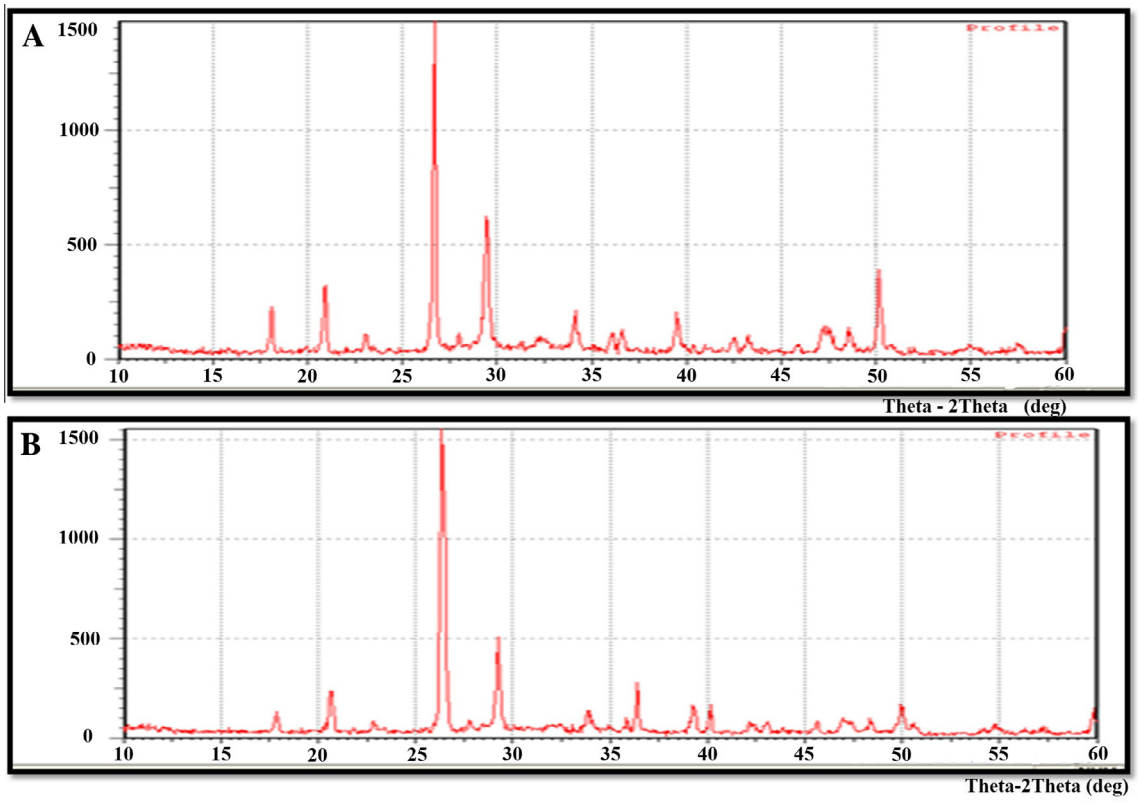

Fig. 7. XRD profile of mortars, (A) CH peaks before adding NS and (B) after adding NS.

3.3. Compressive and tensile strength development

3.3.1. Compressive strength

3.3.1.1. Effect of age on compressive strength. Concerning the tests, the effect of age on compressive strength for control mixture, and NS mixtures, it can be concluded from Fig. 8, that the compressive strength consistently increases with the increase in age for all mortar mixtures. Also, it can be seen from the same figure that the mortar mixture NS6 (30–100) has achieved the highest strength at all ages which confirms the fact that compressive strength of mortar increases with both increasing the percentage of NS to optimum percentage and decreasing the NS particle size. Another observation that is clear is that adding NS is better than without. An example of the previous conclusion is that, at the age of 14 days

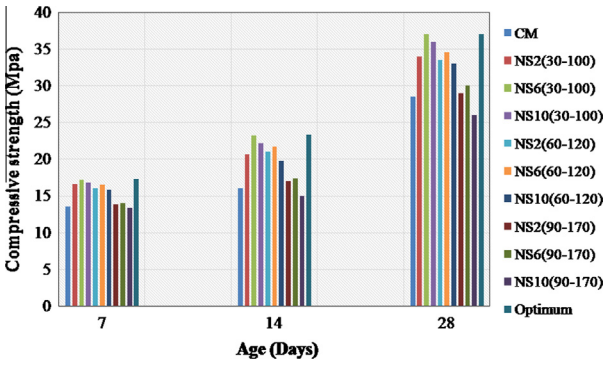

Fig. 8. Effect of age on compressive strength.

the mixture NS6 (30–100) recorded a strength of 23.2 MPa, where the (CM) mixture gave a strength of 16 MPa at the same age. This early strength effect of NS is due to its influence on accelerating the pozzolanic transformation of C_3S, C_2S and CH into the C–S–H gel which is responsible for giving the mortar its strength. Gaining NS enormous early strength is also attributed to the high packing efficiency of nano-particles.

3.3.1.2. Effect of particle size of (NS) on compressive strength development. The variation in the results seems to be a function of the particle size. For instance, the compressive strength of mixture NS6 (30–100) nm had 37 MPa at 28 days slumped to 34.5 MPa for mixture of NS6 (60–120) nm and the mixture NS10 (60–120) nm had 33 MPa dropped to 26 MPa for mixture of NS10 (90–170) nm at the same age and percentage as shown in Fig. 9A–C. A fair explanation for this trend is that as the particle size of NS increases the packing efficiency decreases leading to a drop in the compressive strength. This effect of NS particle size on compressive strength can also be attributed to the large surface area that is available for pozzolanic reaction. That is why in the case of small particle size of NS, more C–S–H is produced and thus its concentration in the mixture increases, leading to a rise in compressive strength. It can be observed from the results that the surface area decreases with the increase in the particle size as in other mixtures of NS and as in the (CM) mixtures which yielded less compressive strength at the same age.

3.3.1.3. Effect of (NS) dosage on compressive strength development of mortars. Compressive strength development of the cement mortars incorporating different dosages of NS is given in Fig. 10A–C. In comparison with that of control Portland cement mortar, the mortar with NS had higher compressive strengths than the Portland cement mortar of 1–28 days as expected. However, the strength of the mortars increased with the increase in NS dosages to optimum value up to 28 days. By examining the strength of the mortar prepared in different percentages of NS for the same particle size, it can be seen from Fig. 10, this mortar mixtures with percentage of NS (6%) displays higher compressive strength than their counterparts prepared with low NS percentage which is the same result as that in the study conducted by Said and Zeidan [18]. For example, the mortar with NS of nominal particle size NS2 (30–100) nm exhibited a compressive strength of 34 MPa at 28 days and 2% NS, while it recorded 37 MPa at 6% NS at the same age. Conversely, a different observation was detected for mixtures which incorporated NS of nominal particle size of NS6 (90–170) nm where the compressive strength result was 6% and at age of 28 days was 30 MPa, while NS10 (90–170) slumped to 26 MPa and mixture NS6 (60–120) nm where the compressive strength result was at 6% and 14 days was 21.7 MPa while NS10 (60–120) nm dropped to 19.8 MPa. This means that increasing the percentage of NS is useful in increasing strength to a certain limit after which any increase in the NS percentage leads to a decrease in the compressive strength. These results are in good agreement with the results obtained by Haruehansapong et al. [19].

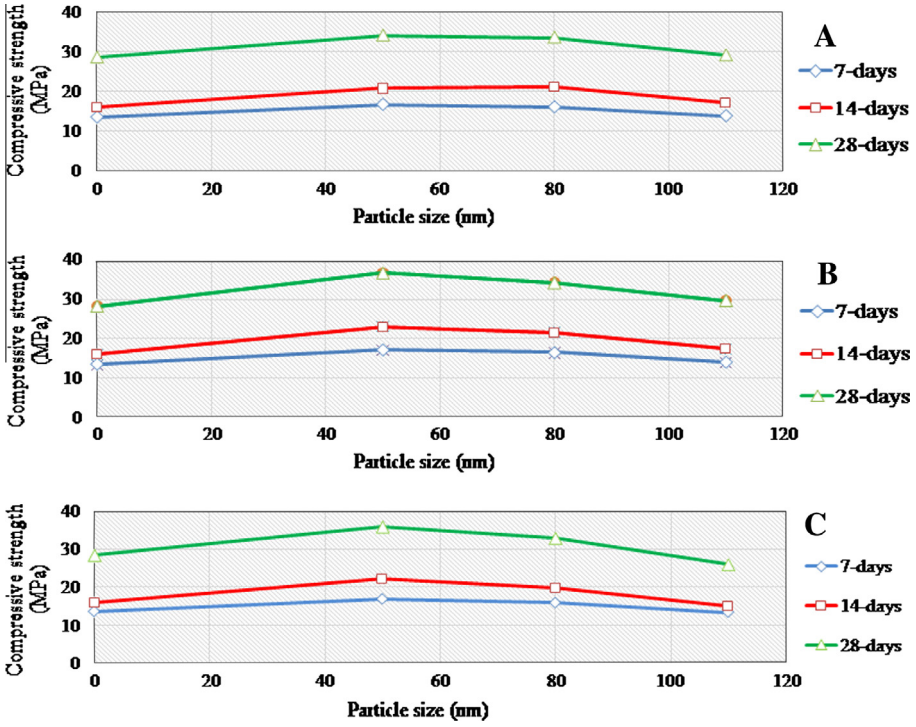

Fig. 9. Effect of particle size of NS on compressive strength for A (2%), B (6%) and C (10%) of NS adding percentages.

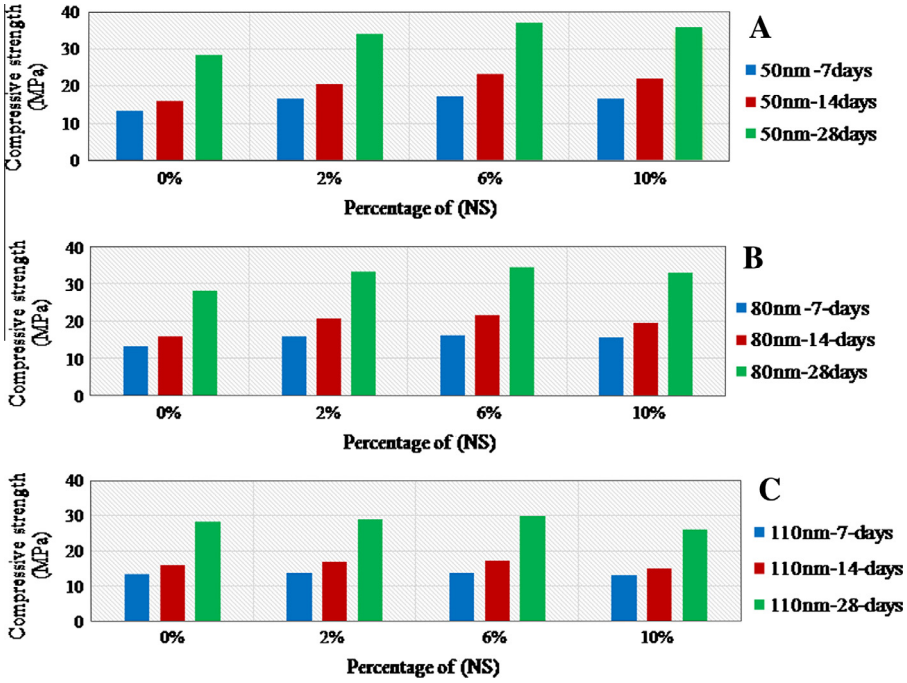

Fig. 10. Effect of NS percentage on compressive strength for: A (50 nm), B (80 nm), and C (110 nm) NS particle size.

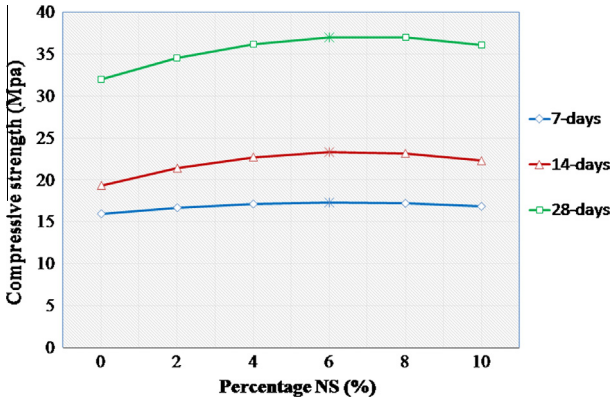

Fig. 11. Compressive strength optimization results for 50 nm particle size.

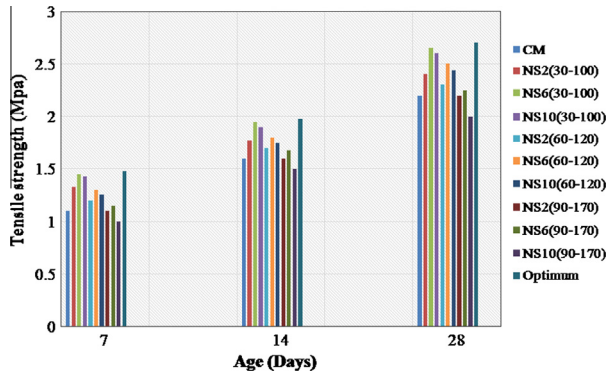

Fig. 12. Effect of age on tensile strength.

3.3.2. Tensile strength development

3.3.2.1. Effect of age on tensile strength. It can be seen from Fig. 12 that adding NS to mortar increases the tensile strength of the specimens at inconsistent rates which matches the results of Li et al. [20]. Concerning tests, the effect of age on tensile strength of control mixture, and NS mixtures, it can be concluded from the same figure that the tensile strength consistently increases with the increase in age for all mortar mixtures. In the course of work on this test a similar problem was faced as with the compressive strength test specifically with mixtures produced by NS of nominal size (90–170) nm. The problem is the low strength results obtained by these mixtures which were even equal to the strength results of conventional mortar mixture. The reason as mentioned before behind these low results is the extra amount of water that was added to those mixtures causing the large number and the large size of voids to negatively affect its strength. It can also be seen in Fig. 12 that some NS mixtures display the same strength as the control mixture as it was the case in the mixtures NS2 (90–170), that displayed a tensile strength of 2.2 MPa. The highest tensile strength attained was by mixture NS6 (30–100) which recorded a tensile strength of 2.65 MPa at the age of 28 days. It could be concluded that adding optimum percentage of NS to mortar mixtures increases its tensile strength and that NS is better than (CM) in enhancing tensile strength. The reason behind that is the large surface area of NS which promotes the pozzolanic reaction to form C–S–H gel which in turn gives the mixture its strength and the micro-filling effect of nano particles that fill the voids and pores of mortar with the small sized nano particles.

3.3.2.2. Effect of particle size of (NS) on tensile strength development. It is shown in Fig. 13A–C that the theory of the increase in compressive strength with the decrease in NS particle size can also be applied to tensile strength. For example, for the NS6 (30–100) group, the tensile strength displayed by mortar prepared with NS of nominal particle size (30–100) nm was 2.65 MPa which slumped to 2.5 MPa for NS nominal particle size NS6 (60–120) nm at the same percentage and age of 28 days. This phenomenon is also due to the higher packing efficiency of small particle size of NS as it was the case in the compressive strength. This trend also comes from the high surface area of small particle size of NS which is more efficient in promoting pozzolanic

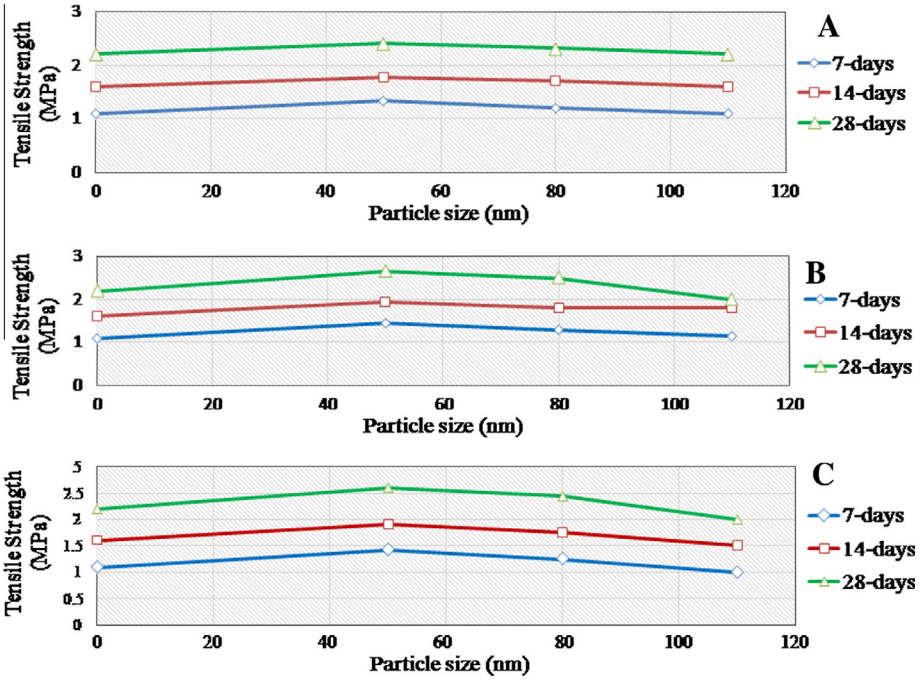

Fig. 13. Effect of particle size of NS on tensile strength for A (2%), B (6%), and C (10%) NS.

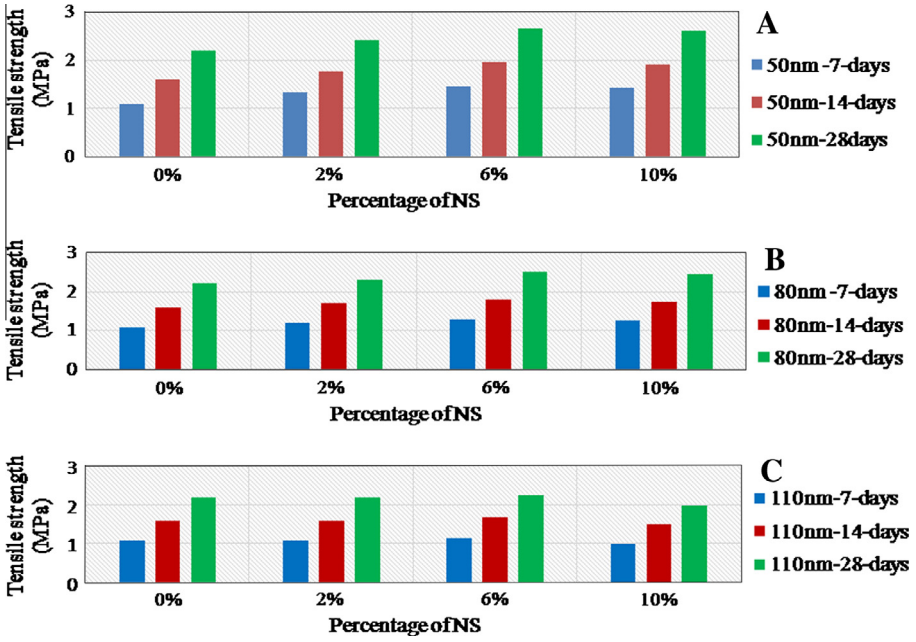

Fig. 14. Effect of (NS) percentage on tensile strength for A (50 nm), B (80 nm) and C (110 nm) NS.

Table 4
Multiple regression analysis results for compressive strength.

Property	Regression coefficients						Goodness of fit analysis			
	a_0	a_1	a_2	a_3	a_4	a_5	Corr. coeff. (R)	Variance Explained (%)	Mean abs. error	Mean square error
Compressive strength 7-days	13.49066	0.495973	0.091681	−0.001380	−0.033913	−0.000855	0.99969	99.937	0.030361	0.001334
Compressive strength 14-days	1.604717	0.130407	0.000989	−0.000456	−0.007629	−0.000021	0.99134232	98.27596	0.014982	0.000348
Compressive strength 28-day	28.33313	1.937580	0.137206	−0.009026	−0.107368	−0.001291	0.99416	98.836	0.316884	0.132222

Table 5
Multiple regression analysis results for tensile strength.

Property	Regression coefficients						Goodness of fit analysis			
	a_0	a_1	a_2	a_3	a_4	a_5	Corr. coeff. (R)	Variance Explained (%)	Mean abs. error	Mean square error
Tensile strength 7-days	1.107525	0.117454	0.002210	−0.000459	−0.006518	−0.000031	0.99070	98.149	0.016855	0.000404
Tensile strength 14-days	1.604717	0.130407	0.000989	−0.000456	−0.007629	−0.000051	0.99134232	98.27596	0.014982	0.000348
Tensile strength 28-days	2.189175	0.178180	0.000931	−0.000743	−0.009464	−0.000022	0.98525685	97.073106	0.027161	0.001163

Table 6
ANOVA analysis for compressive strength results.

Source of variance	SS	dF	MS	F	P	R^2	$R^2_{adjusted}$
Compressive strength 7-day							
Regression model SS_R	21.1306	5	4.2261	126.784	0.000171	0.99373	0.98589
Error (residual) SS_E	0.1333	4	0.0333				
Total SS_T	21.2639	9	4.2594				
Compressive strength 14-day							
Regression model SS_R	70.9493	5	14.1898	14.8326	0.010877	0.94882	0.88485
Error (residual) SS_E	3.82666	4	0.95666				
Total SS_T	74.7759	9	15.1464				
Compressive strength 28-day							
Regression model SS_R	106.8477	5	21.3695	12.6198	0.014631	0.940387	0.86587
Error (residual) SS_E	6.77333	4	1.69333				
Total SS_T	113.6210	9	23.0628				

Table 7
ANOVA analysis for tensile strength results.

Source of variance	SS	dF	MS	F	P	R^2	$R^2_{adjusted}$
Tensile strength 7-day							
Regression model SS_R	0.20699	5	0.041399	14.4696	0.011386	0.947608	0.882119
Error (residual) SS_E	0.01144	4	0.002861				
Total SS_T	0.21843	9	0.04426				
Tensile strength 14-day							
Regression model SS_R	0.18916	5	0.037833	11.7819	0.016576	0.936417	0.856938
Error (residual) SSE	0.01284	4	0.003211				
Total SS_T	0.202	9	0.041044				
Tensile strength 28-day							
Regression model SS_R	0.34902	5	0.069805	5.78492	0.056911	0.878510	0.726648
Error (residual) SS_E	0.04826	4	0.012067				
Total SS_T	0.39728	9	0.081872				

reaction as explained before in the compressive strength section. Also, this high activity of small particles increases the bond between the sand and the cement matrix and this bond is the most effective factor in increasing the tensile strength of the mortar. Generally, the tensile strength increases with the decrease in the particle size of NS which makes adding NS give better tensile strength results.

3.3.2.3. Effect of (NS) dosage on tensile strength development. Fig. 14 shows the trend of increased tensile strength with the increase in the NS percentage to optimum value. By examining the tensile strength of the mortar prepared in different percentages of NS for the same particle size, it can be seen from results that the mortar mixtures with percentage of NS (6%) displays higher tensile strength than other specimens.

3.4. Optimization results

The results of multiple regression analysis of the developed model equations and goodness of fit analysis were estimated using STATISTICA software and have been illustrated in Tables 4 and 5. The model results are in good accordance with experimental measurements as verified by analysis of variance (ANOVA). The ANOVA results are explained in Tables 6 and 7, the results show higher values of model R^2 than adjusted R^2 for all cases studied which proved the statistical acceptance of the model. Tables 8 and 9, show the optimum conditions obtained using WinQSB technique. Figs. 11 and 15 show the optimum conditions of compressive and tensile strengths respectively. Optimization results have proved that an improvement in compressive strength of 29.889% takes place under optimum conditions of (6% NS adding percent and 50 nm particle size) in 28 day age, while for tensile strength is 22.863%

Table 8
Optimum condition results for compressive strength.

Age	Optimum conditions		
	X_1 (%)	X_2 (nm)	Y_{max}
At 7-days	6	50	17.2782
At 14-days	6	50	23.3354
At 28-days	6	50	37.0184

Table 9
Optimum condition results for tensile strength.

Age	Optimum conditions		
	X_1 (%)	X_2 (nm)	Y_{max}
7-days	8	50	1.4794
14-days	8	50	1.9743
28-days	8	50	2.7033

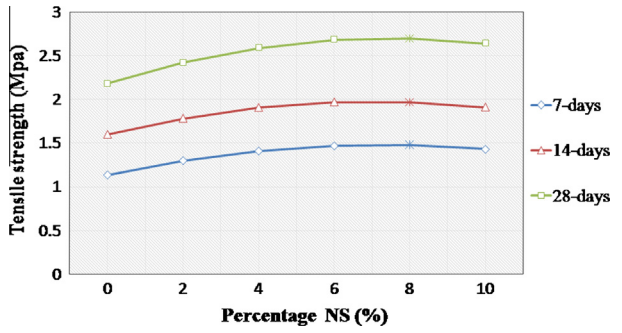

Fig. 15. Tensile strength optimization results for 50 nm particle size.

at optimum conditions of (8% NS adding percent and 50 nm particle size) in 28 day age. These results are comparable to those obtained by Ammar [21].

4. Conclusions

From this work, the following main conclusions are drawn:

1. Nano-silica was successfully obtained by (Ball milling) method for (30–50) hours with average particle size of 50 nm.
2. The characterization of (NS) shows (NS) are spherical particles and have irregular shapes as well as agglomerates fuse together and the range of external diameters is (30–100) nm.
3. Incorporating nano-silica into cement mortar mixtures enhances their mechanical properties, by yielding higher compressive and tensile strengths than control mixture, and exhibit relatively high early strengths.
4. Within the particle size and dosage range examined at all curing ages, the strength generally increases with the addition of NS, the optimum percentage of NS is (6%) for compressive strength, (8%) for tensile strength, and 50 nm particle size gives the highest the strength of cement mortar mixtures, optimization results proved an improvement in compressive strength of 29.889% under optimum conditions at 28 day age, while for tensile strength is 22.863% under optimum conditions at 28 day age.

Acknowledgments

The authors would like to thank everyone who has helped to complete this work, especially, Dr. Flaeh Hassan Fadhil from the Ministry of Science and Technology, Baghdad-Iraq, for his contribution to testing and measurements.

References

[1] K.L. Scrivener, R.J. Kirkpatrick, Innovation in use and research on cementious material, Cem. Concr. Res. 38 (2008) 128–136.
[2] H.G. Li Hui, J. Xiao, Jie, J.P. Ou, Microstructure of cement mortar with nano-particles, Compos. B Eng. 35 (2) (2004) 185–189.
[3] Q. Ye, Z.N. Zhang, R.S. Chen, C.C. Ma, Interaction of nano-SiO_2 with calcium hydroxide crystals at interface between hardened cement paste and aggregate, J. Chin. Ceram. Soc. 31 (5) (2003) 517–522.
[4] A. Mahamat, A. Rani, P. Husain, Behavior of Cu–WC–Ti metal composite after using planetary ball milling, Int. Eng. Appl. Sci. (2012) 278–282.
[5] Y. Wang, E. Forssberg, Production of carbonate and silica nano-particles in stirred bead milling, Int. J. Miner. Process. 81 (1) (2006) 1–14.
[6] M. Hubert, E. Petracovschi, X.-H. Zhang, L. Calvez, Synthesis of germanium–gallium–tellurium (Ge–Ga–Te) ceramics by ball-milling and sintering, J. Am. Ceram. Soc. 96 (5) (2013) 1444–1449.
[7] P. Alvarez, J.L.S. Llamazares, M.J. Pérez, et al., Microstructural and magnetic characterization of Nd_2Fe_{17} ball milled alloys, J. Non-Cryst. Solids 354 (47–51) (2008) 5172–5174.
[8] ASTM C (109-08), Standard Test Method for Compressive Strength of Hydraulic Cement Mortars, ASTM International, 2008.
[9] ASTM C (780-002), Standard Test Method for Preconstruction and Construction Evaluation of Mortars for Plain and Reinforced Unit Masonry, Annual Book of ASTM Standards, vol. 04-02, 2004.
[10] A. Wahyudia, T. Nurasidb, S. Rochania, Preparation of nanoparticle silica from silica sand and quartzite by ultrafine grinding, in: Proceeding of International Conference, 28, 2012, pp. 1–7.
[11] T. Ahmad, O. Mamat, The development and characterization of zirconia-silica sand nanoparticles composites, World J. Nano Sci. Eng. 1 (2011) 7–14.
[12] Y. Wang, E. Forssberg, Production of carbonate and silica nano-particles in stirred bead milling, Int. J. Miner. Process 81 (2006) 1–14.
[13] G. Quercia, A. Lazaro, J.W. Geus, H.J.K. Brouwers, Characterization of morphology and texture of several amorphous nano-silica particles used in concrete, Cement Concr. Compos. (2013) 45.
[14] L.P. Singh, S.K. Agarwal, S.K. Bhattacharyya, U. Sharma, S. Ahalawat, Preparation of silica nanoparticles and its beneficial role in cementitious materials, Nanomater. Nanotechnol. 1 (1) (2011) 44–51.
[15] J. Belkowitz, D. Armentrout, An Investigation of Nano Silica in the Cement Hydration Process, ACI, SP267-08, October 2009, pp. 87–100.
[16] G. Quercia, Spiesz, G. Hüsken, H.J.H. Brouwers, SCC Modification by use of amorphous nano-silica, Cement Concr. Compos. 45 (2014) 69–81.
[17] M. Aly, M.S.J. Hashmi, A.G. Olabi, M. Messeiry, E.F. Abadir, A.I. Hussain, Effect of colloidal nano-silica on the mechanical and physical behavior of waste-glass cement mortar, Mater. Des. 33 (2012) 127–135.
[18] A. Said, M. Zeidan, Enhancing the Reactivity of Normal and Fly Ash Concrete Using Colloidal Nano-silica, ACI, SP267-07, 2009, pp. 75–86.
[19] S. Haruehansapong, T. Pulngern, S. Chucheepsakul, Effect of the particle size of nano-silica on the compressive strength and the optimum replacement content of cement mortar containing nano-SiO_2, Constr. Build. Mater. 50 (2014) 471–477.
[20] H. Li, H. Xiao, J. Yuan, J. Ou, Microstructure of cement mortar with nano-particles, Compos. B Eng. 35 (2) (2004) 185–189.
[21] M.M.A.H. Ammar, The effect of nano-silica on the performance Of Portland Cement Mortar, MSc, Thesis, The American University in Cairo, 2012.